AEM
Journals.ASM.org

Benchmarking Various Green Fluorescent Protein Variants in *Bacillus subtilis*, *Streptococcus pneumoniae*, and *Lactococcus lactis* for Live Cell Imaging

Wout Overkamp,[a,b] Katrin Beilharz,[a] Ruud Detert Oude Weme,[a] Ana Solopova,[a] Harma Karsens,[a] Ákos T. Kovács,[a]* Jan Kok,[a] Oscar P. Kuipers,[a,b] Jan-Willem Veening[a]

Department of Molecular Genetics, Groningen Biomolecular Sciences and Biotechnology Institute, Centre for Synthetic Biology, University of Groningen, Groningen, The Netherlands[a]; Kluyver Centre for Genomics of Industrial Fermentation, Delft, The Netherlands[b]

Green fluorescent protein (GFP) offers efficient ways of visualizing promoter activity and protein localization *in vivo*, and many different variants are currently available to study bacterial cell biology. Which of these variants is best suited for a certain bacterial strain, goal, or experimental condition is not clear. Here, we have designed and constructed two "superfolder" GFPs with codon adaptation specifically for *Bacillus subtilis* and *Streptococcus pneumoniae* and have benchmarked them against five other previously available variants of GFP in *B. subtilis*, *S. pneumoniae*, and *Lactococcus lactis*, using promoter-*gfp* fusions. Surprisingly, the best-performing GFP under our experimental conditions in *B. subtilis* was the one codon optimized for *S. pneumoniae* and *vice versa*. The data and tools described in this study will be useful for cell biology studies in low-GC-rich Gram-positive bacteria.

The use of *Aequorea victoria* green fluorescent protein (GFP) and its derivatives has tremendously increased our knowledge of bacterial cell biology (1, 2). Because of the possibilities to examine protein localization or gene expression in live cells, new improved variants of GFP appear regularly. However, *in vivo* benchmarking to demonstrate which GFP variant is best suited for which organism and experimental setup is scarce. Here, we benchmark a set of commonly used GFP variants to analyze gene expression in the low-GC-rich Gram-positive model organisms *Bacillus subtilis*, *Streptococcus pneumoniae*, and *Lactococcus lactis*.

Bacillus subtilis is one of the best-studied microorganisms that is able to differentiate into distinct cell types. It can form highly resistant spores, develop natural competence and motility, and secrete exoproteases (3–7). Additionally, it can form biofilms (8) for which, due to poor aeration, not all GFP variants might be suitable, since maturation of GFP requires posttranslational oxidation. *Streptococcus pneumoniae* is a major pathogen causing pneumonia, meningitis, and other diseases in young children, elderly, and immunocompromised adults (9, 10). More recently, *S. pneumoniae* turned out to be an excellent model to study cell biology in oval-shaped bacteria (11–14). *Lactococcus lactis* is an industrially important lactic acid bacterium. Because of its ability to acidify milk products, *L. lactis* is extensively used in cheese starter cultures. Both *S. pneumoniae* and *L. lactis* are microaerophiles, and it is not clear which GFP variants are most suitable under such low-oxygen conditions.

GFP offers efficient ways of visualizing gene expression and protein targeting. It exhibits intrinsic fluorescence and is commonly used as a reporter gene in intact cells and organisms (1, 15–17). For *in vivo* studies of weakly expressed genes, a strong GFP fluorescence signal is crucial. Since the initial publication of *A. victoria* GFP and its application for molecular biology (16), many mutants of the protein with either modified spectral properties, increased fluorescence intensity, or improved folding properties have been reported (18–21). The number of possible applications for GFP has increased, but the most suitable candidate remains to be selected carefully for the particular research question at hand. The suitability of a certain GFP variant for a specific experiment strongly depends on factors such as availability of oxygen, cultivation temperature, pH of the environment, photostability, spectral overlap, toxicity, and multimerization (21).

Methods to achieve the most optimal fluorescence signal are not limited to modifications on the protein level. Important factors influencing protein expression levels besides transcription rate are mRNA stability, translation signals, and codon usage in the gene (22). For instance, highly expressed prokaryotic genes have a pronounced codon usage bias, significantly different from genes expressed at low levels (23). Adaptation of the *gfp* gene to the typical codon usage of the host could have a major impact on its translation, resulting in more efficient protein production and folding, resulting in higher net GFP expression and thus fluorescence signal (24). The three low-GC model organisms described above vary slightly in codon usage, and therefore a different *gfp* variant might be optimal in each of the species (see Table S1 in the supplemental material). The GFP variants characterized in this paper have all proven to be successful in molecular biology. However, knowing which GFP variant gives the most optimal fluores-

Received 26 June 2013 Accepted 7 August 2013
Published ahead of print 16 August 2013
Address correspondence to Jan-Willem Veening, j.w.veening@rug.nl, or Oscar P. Kuipers, o.p.kuipers@rug.nl.
* Present address: Ákos T. Kovács, Terrestrial Biofilms Group, Institute of Microbiology, Friedrich Schiller University of Jena, Jena, Germany.
K.B., R.D.O.W., A.S., and H.K. contributed equally to this article.
Supplemental material for this article may be found at http://dx.doi.org/10.1128/AEM.02033-13.

doi:10.1128/AEM.02033-13

cence signal in each of the three model organisms would be very helpful in optimizing experimental setups.

In this work, we focused on benchmarking GFP for studying gene expression at the single-cell level. Previously characterized promoters and ribosome binding sites were used to drive GFP expression. To assess gene activation accurately, it is important that the fluorescent signal appears immediately after induction. Therefore, we have also employed fast folding variants such as GFP+ (20) and superfolder GFP (19) and designed and generated vectors containing superfolder GFPs with codon usage adapted specifically for *B. subtilis* or *S. pneumoniae*. Interestingly, superfolder GFP did not give the highest fluorescence signals in *B. subtilis* liquid cultures and biofilms, but gave the highest fluorescence signals in both *S. pneumoniae* and *L. lactis*. More surprisingly was the finding that *gfp* codon optimized for *S. pneumoniae* worked best in *B. subtilis* and *vice versa*. Together we provide a new GFP toolbox and knowledge as to which GFP variant to use for single-cell gene expression analysis in *B. subtilis*, *S. pneumoniae*, and *L. lactis*.

MATERIALS AND METHODS

Bacterial strains, plasmids, media, and growth conditions. Bacterial strains and plasmids used in this study are listed in Table 1. *Bacillus subtilis* was grown at 37°C on LB (25) solidified with 1.5% (wt/vol) agar or in liquid LB or Spizizen minimal medium (26) with shaking at 200 rpm (see below). For induction of the $P_{hyperspank}$ promoter, 0.1 mM isopropyl-β-D-1-thiogalactopyranoside (IPTG) was used. For architecturally complex colonies, *B. subtilis* strains were grown on 2× SG medium [16 g/liter of nutrient broth (Difco), 2 g/liter KCl, 0.5 g/liter $MgSO_4 \cdot 7H_2O$, 1 mM $Ca(NO_3)_2$, 0.1 mM $MnCl_2 \cdot 4H_2O$, 1 μM $FeSO_4$, and 0.1% glucose] solidified by 1.5% agar (27).

Streptococcus pneumoniae was grown as standing cultures at 37°C in C+Y medium (28). Blood agar plates were made from Columbia agar containing 3% defibrinated sheep blood (Johnny Rottier, Kloosterzade, The Netherlands). For induction of the P_{Zn} promoter, 0.1 mM $ZnCl_2$ was added to liquid medium.

Lactococcus lactis was grown as standing cultures at 30°C in M17 broth (Difco, Sparks, MD) containing 0.5% (wt/vol) glucose.

Escherichia coli DH5α or EC1000 was used as the host for cloning and grown in LB medium at 37°C with shaking or on LB medium solidified with 1.5% (wt/vol) agar. When required, the growth media were supplemented with the following antibiotics: 100 μg ml^{-1} ampicillin (Amp) or 150 μg ml^{-1} erythromycin (Em) for *E. coli*, 100 μg ml^{-1} spectinomycin (Spec) for *B. subtilis*, 1 μg ml^{-1} tetracycline (Tet) for *S. pneumoniae*, and 3 μg ml^{-1} erythromycin for *L. lactis*.

Recombinant DNA techniques and oligonucleotides. Procedures for DNA isolation, restriction, ligation, agarose gel electrophoresis, and transformation of *E. coli* were performed as described by Sambrook et al. (25). Plasmid DNA and PCR products were isolated and purified using the high pure plasmid isolation kit (Roche Applied Science, Mannheim, Germany) according to the manufacturer's instructions. Enzymes were purchased from New England BioLabs (Ipswich, MA, USA) and Fermentas (Vilnius, Lithuania) and used as described by the manufacturer. For PCR amplification, Phusion and *Taq* DNA polymerase (Fermentas) were used. *B. subtilis* was transformed as described by Harwood and Cutting (29). *S. pneumoniae* was transformed as described by Martin et al. (28). *L. lactis* was transformed as described by Holo and Nes (30). Oligonucleotides used in this study are listed in Table S2 in the supplemental material and were purchased from Biolegio (Nijmegen, The Netherlands).

Codon optimization. To design a gene encoding superfolder GFP (19) that is codon optimized for *S. pneumoniae*, we employed OPTIMIZER (31) using the genome of *S. pneumoniae* R6 as the reference and ensured that rare codons would never be used. Next, we ran simulations to generate more than 1,000 solutions of superfolder *gfp* with the desired codon usage (codon usage similar to that of highly expressed genes) and selected the variant with the lowest free energy (ΔG°) value in mRNA secondary structure around the ribosome binding site (RBS) that potentially improves translation (32), and this gene was synthesized (Genscript USA Inc., Piscataway, NJ, USA) and called *sfgfp*(*Sp*) [named *sfgfp*(*Sp*) for superfolder GFP that is codon optimized for *S. pneumoniae*]. The sequence for a codon-harmonized variant for *Bacillus subtilis* codon usage was obtained from DSM Biotechnology Center (Delft, The Netherlands) and is called *sfgfp*(Bs) in this work.

Construction of plasmids. To construct derivatives of plasmid pDR111 (33) for *B. subtilis*, each carrying a variant of the *gfp* gene, a PCR with the primers GFP_NheI_fw (fw stands for forward) and GFP_SphI_rv (rv stands for reverse) was performed using plasmids pKB01_gfpmut1, pKB01_gfp+, pKB01_gfp+htrA, pKB01_gfp(Sp), pKB01_sfgfp(Bs), pKB01_sfgfp(Sp), and pKB01_sfgfp(iGEM) as the templates. The amplified fragments were subsequently cleaved with NheI and SphI and ligated separately in pDR111 digested with the same enzymes to generate plasmids pDR111_gfpmut1, pDR111_gfp+, pDR111_gfp+htrA, pDR111_gfp(Sp), pDR111_sfgfp(Bs), pDR111_sfgfp(Sp), and pDR111_sfgfp(iGEM).

To construct plasmid pJWV100 for *S. pneumoniae*, a sequence containing *S. pneumoniae*-codon-optimized superfolder *gfp* gene [*sfgfp*(Sp)], flanked by transcription terminators (one before *gfp* preventing incoming read-through transcription and three after *gfp* to stop *gfp* transcription and prevent incoming, antisense transcription), was designed and synthesized (Genscript USA Inc., Piscataway, NJ, USA) resulting in plasmid pUC57-gfp_sf. The included transcription terminator upstream of the *gfp* gene originates from *S. pneumoniae rpsD* (AAGCACTTTGGGACGTTC TCCCTTAGTGCTTTTTTGATTTCTC), and the ones downstream are from *B. subtilis rrnB* (TAGGACGCCGCCAAGCCAGCTTAAACCCAGC TCAATGAGCTGGGTTTTTTGTTAAAAATGAAGAAGAAACTGTGA AGCGTATTTA), *S. pneumoniae rpsI* (AAAGCACTCAAAAGTTTACCT TATGGGTGCTTTTTTCGTGCTTTTTTGAAAA), and *S. pneumoniae tufA* (AAAAAAAGAACCTTGCCAAGCAAGATTC). This construct was liberated using the restriction enzymes SphI and BlpI and inserted in similarly digested pPP2 (34), thereby replacing *lacZ* with *sfgfp*(Sp) resulting in plasmid pJWV100. To construct plasmid pKB01_sfgfp(Sp) for *S. pneumoniae*, the zinc-inducible promoter P_{Zn} was amplified from chromosomal DNA of *S. pneumoniae* D39 using the primers PczcD-F+FseI (F stands for forward) and PczcD-R+EcoRI (R stands for reverse). The amplicon was digested with restriction enzymes FseI and EcoRI and ligated into similarly cut pJWV100. To construct derivatives of plasmid pKB01_sfgfp(Sp) carrying different *gfp* variants, the corresponding *gfp* genes were amplified by PCR using the appropriate plasmid as the template. The *gfpmut1* gene was amplified from pSG1151 (35) using the primers gfp-mut1-F+XbaI and gfp-mut1-R+SpeI. To obtain *gfp*+ and *htrA′-gfp*+, the plasmid pJWV25 (12) was used as the template with the primer pairs gfp+-F+XbaI/gfp+-R+SpeI and gfp+-F-htrA+XbaI/gfp+-R+SpeI, respectively. The *gfp*(*Sp*) gene was amplified from pUC57-gfp(opt) (36) using the primers gfp-nath-F+XbaI and gfp-nath-R+SpeI. The gene encoding sfGFP(iGEM) (superfolder GFP designed for the International Genetically Engineered Machine competition [iGEM] in 2008) was amplified from pSB1A2-BBa_I746909 (37) using gfp_sf-ori-F+XbaI and gfp_sf-ori-R+SpeI as primers. The PCR fragments were digested using restriction enzymes XbaI and SpeI. The *sfgfp*(Bs) gene was liberated from pMA-gfpDSM (synthesized by GeneArt [Regensburg, Germany]) using the restriction enzymes XbaI and SpeI. The DNA fragments obtained were ligated into the corresponding sites of similarly digested pKB01_sfgfp(Sp), thereby replacing the *sfgfp*(Sp) gene, yielding plasmids pKB01_gfpmut1, pKB01_gfp+, pKB01_gfp+htrA, pKB01_gfp(Sp), pKB01_sfgfp(iGEM), and pKB01_sfgfp(Bs).

Plasmids for *L. lactis* were constructed as follows. The *gfpmut1* gene was amplified by PCR with primer pair gfp_F/gfp_R using pKB01_gfpmut1 as the template. The amplicon was inserted in *L. lactis* integration vector pSEUDO-GFP (38) as an XhoI/BamHI restriction fragment replacing the resident *gfp-sf* gene. This yielded the pSEUDO-gfpmut1. P*usp45* was amplified using primers Pusp45XhoIR and

TABLE 1 Bacterial strains and plasmids used in this study

Bacterial strain or plasmid	Relevant characteristic(s)	Source or reference
E. coli DH5α	F$^-$ *araD139* Δ(*ara-leu*)*7696* Δ(*lac*)*X74 galU galK hsdR2 mcrA mcrB1 rspL*	Laboratory stock
B. subtilis strains		
168	*trpC2*	39
168_gfpmut1	168 *amyE*::P$_{hyperspank}$-*gfpmut1*; Sp^r	This study
168_gfp+	168 *amyE*::P$_{hyperspank}$-*gfp*+; Sp^r	This study
168_gfp+htrA	168 *amyE*::P$_{hyperspank}$-*gfp*+(*htrA*); Sp^r	This study
168_gfp(Sp)	168 *amyE*::P$_{hyperspank}$-*gfp*(*Sp*); Sp^r	This study
168_sfgfp(Bs)	168 *amyE*::P$_{hyperspank}$-*sfgfp*(*Bs*); Sp^r	This study
168_sfgfp(Sp)	168 *amyE*::P$_{hyperspank}$-*sfgfp*(*Sp*); Sp^r	This study
168_sfgfp(iGEM)	168 *amyE*::P$_{hyperspank}$-*sfgfp*(*iGEM*); Sp^r	This study
S. pneumoniae strains		
R6	D39 (Δ*cps2* [nt 2538-9862 deleted]); nonencapsulated	40
KB1-7	R6 *tet bga*::P$_{Zn}$-*gfpmut1*	This study
KB1-5	R6 *tet bga*::P$_{Zn}$-*gfp*+	This study
KB1-6	R6 *tet bga*::P$_{Zn}$-*gfp*+(*htrA*)	This study
KB1-8	R6 *tet bga*::P$_{Zn}$-*gfp*(*Sp*)	This study
KB1-9	R6 *tet bga*::P$_{Zn}$-*sfgfp*(*Bs*)	This study
KB1-3	R6 *tet bga*::P$_{Zn}$-*sfgfp*(*Sp*)	This study
KB1-4	R6 *tet bga*::P$_{Zn}$-*sfgfp*(*iGEM*)	This study
L. lactis subsp. *cremoris* strains		
MG1363	Plasmid-free derivative of NCDO712 (Prt$^-$ Lac$^-$)	56
MG_gfpmut1	MG1363 pseudo 10 gene::P*usp45-gfpmut1*; Ery^r	This study
MG_gfp+	MG1363 pseudo 10 gene::P*usp45-gfp*+; Ery^r	This study
MG_gfp+htrA	MG1363 pseudo 10 gene::P*usp45-gfp*+(*htrA*); Ery^r	This study
MG_gfp(Sp)	MG1363 pseudo 10 gene::P*usp45-gfp*(*Sp*); Ery^r	This study
MG_sfgfp(Bs)	MG1363 pseudo 10 gene::P*usp45-sfgfp*(*Bs*); Ery^r	This study
MG_sfgfp(Sp)	MG1363 pseudo 10 gene::P*usp45-sfgfp*(*Sp*); Ery^r	This study
MG_sfgfp(iGEM)	MG1363 pseudo 10 gene::P*usp45-sfgfp*(*iGEM*); Ery^r	This study
Plasmids		
pDR111	*bla amyE*′ P$_{hyperspank}$ *spec lacI* ′*amyE*	Gift of D. Rudner
pDR111_gfpmut1	*bla amyE*′ P$_{hyperspank}$-*gfpmut1 spec lacI* ′*amyE*	This study
pDR111_gfp+	*bla amyE*′ P$_{hyperspank}$-*gfp*+ *spec lacI* ′*amyE*	This study
pDR111_gfp+htrA	*bla amyE*′ P$_{hyperspank}$-*gfp*+(*htrA*) *spec lacI* ′*amyE*	This study
pDR111_gfp(Sp)	*bla amyE*′ P$_{hyperspank}$-*gfp*(*Sp*) *spec lacI* ′*amyE*	This study
pDR111_sfgfp(Bs)	*bla amyE*′ P$_{hyperspank}$-*sfgfp*(*Bs*) *spec lacI* ′*amyE*	This study
pDR111_sfgfp(Sp)	*bla amyE*′ P$_{hyperspank}$-*sfgfp*(*Sp*) *spec lacI* ′*amyE*	This study
pDR111_sfgfp(iGEM)	*bla amyE*′ P$_{hyperspank}$-*sfgfp*(*iGEM*) *spec lacI* ′*amyE*	This study
pJWV100	*bla tet bgaA sfgfp*(*Sp*)	This study
pKB01_gfpmut1	*bla tet bgaA* P$_{Zn}$-*gfpmut1*	This study
pKB01_gfp+	*bla tet bgaA* P$_{Zn}$-*gfp*+	This study
pKB01_gfp+htrA	*bla tet bgaA* P$_{Zn}$-*gfp*+(*htrA*)	This study
pKB01_gfp(Sp)	*bla tet bgaA* P$_{Zn}$-*gfp*(*Sp*)	This study
pKB01_sfgfp(Bs)	*bla tet bgaA* P$_{Zn}$-*sfgfp*(*Bs*)	This study
pKB01_sfgfp(Sp)	*bla tet bgaA* P$_{Zn}$-*sfgfp*(*Sp*)	This study
pKB01_sfgfp(iGEM)	*bla tet bgaA* P$_{Zn}$-sf*gfp*(*iGEM*)	This study
pSEUDO-gfp	*ery^R* pseudo 10′ gene *gfp-sf* ′pseudo 10 gene	38
pSEUDO::Pusp45-gfpmut1	*ery^R* pseudo 10′ gene P*usp45-gfpmut1* ′pseudo 10 gene	This study
pSEUDO::Pusp45-gfp+	*ery^R* pseudo 10′ P*usp45-gfp*+ ′pseudo 10 gene	This study
pSEUDO::Pusp45-gfp+htrA	*ery^R* pseudo 10′ gene P*usp45-gfp*+(*htrA*) ′pseudo 10 gene	This study
pSEUDO::Pusp45-gfp(Sp)	*ery^R* pseudo 10′ gene P*usp45-gfp*(*Sp*) ′pseudo 10 gene	This study
pSEUDO::Pusp45-sfgfp(Bs)	*ery^R* pseudo 10′ gene *Pusp45-sfgfp*(*Bs*) ′pseudo 10 gene	This study
pSEUDO::Pusp45-sfgfp(Sp)	*ery^R* pseudo 10′ gene *Pusp45-sfgfp*(*Sp*) ′pseudo 10 gene	This study
pSEUDO::Pusp45-sfgfp(iGEM)	*ery^R* pseudo 10′ gene *Pusp45-sfgfp*(*iGEM*) ′pseudo 10 gene	This study

Pusp45SmaIF using *L. lactis* MG1363 chromosomal DNA as the template; the PCR fragment was cloned in pSEUDO-GFPmut1 using XhoI/SmaI. This yielded plasmid pSEUDO::Pusp45-gfpmut1. Genes encoding different GFP variants were obtained by PCR with primer pair gfp_F/gfp_R using vectors pKB01_gfp+, pKB01_gfp+ htrA, pKB01_gfp(Sp), pKB01_sfgfp(Bs), pKB01_sfgfp(Sp), and pKB01_sfgfp(iGEM) as the templates. The PCR fragments were subsequently cloned into pSEUDO::Pusp45-gfpmut1 as XhoI/BamHI restriction fragments replacing the res-

TABLE 2 GFP variants benchmarked in this study

GFP	Changes to *A. victoria* GFP	Properties	Gene codon optimization method	Reference
GFPmut1	F64L, S65T, L195S	35-fold brighter than wild-type GFP	Original codon adaptation from *A. victoria*	18
GFP+	F64L, S65T, Q80R, F99S, M153T, V163A	130-fold brighter than wild-type GFP	*E. coli*	20
GFP+(*htrA*)	M1MKHL, F64L, S65T, Q80R, F99S, M153T, V163A	Improved translation efficiency in *S. pneumoniae*	*E. coli*	12
GFP(*Sp*)	M1MV, S65A, V68L, S72A, A206K	Based on GFPmut2, monomer	*S. pneumoniae* using OptimumGene	36
sfGFP(*Bs*)	S30R, Y39N, F64L, S65T, Q80R, F99S, N105T, Y145F, M153T, V163A, I171V, A206V	Superfolder GFP (19)	*B. subtilis* using dual codon method	This study
sfGFP(*Sp*)	S30R, Y39N, F64L, S65T, Q80R, F99S, N105T, Y145F, M153T, V163A, I171V, A206V	Superfolder GFP (19)	*S. pneumoniae* using OPTIMIZER (55)	This study
sfGFP(iGEM)	S2R, S30R, Y39N, F64L, S65T, S72A, F99S, N105T, Y145F, M153T, V163A, I171V, A206V	Superfolder GFP, additional mut3* mutations	*E. coli* and *B. subtilis*	46

ident *gfpmut1* gene. This yielded vectors pSEUDO::Pusp45-gfp+, pSEUDO::Pusp45-gfp+htrA, pSEUDO::Pusp45-gfp(Sp), pSEUDO::Pusp45-sfgfp(Bs), pSEUDO::Pusp45-sfgfp(Sp), and pSEUDO::Pusp45-sfgfp(iGEM).

Construction of strains. *B. subtilis* strains 168_gfpmut1, 168_gfp+, 168_gfp+htrA, 168_gfp(Sp), 168_sfgfp(Bs), 168_sfgfp(Sp), and 168_sfgfp(iGEM) were obtained by double-crossover recombination events between the chromosomal *amyE* gene of *B. subtilis* 168 (39) and the *amyE* regions on the plasmids pDR111_gfpmut1, pDR111_gfp+, pDR111_gfp+htrA, pDR111_gfp(Sp), pDR111_sfgfp(Bs), pDR111_sfgfp(Sp), and pDR111_sfgfp(iGEM), respectively. Transformants were selected on LB agar plates containing spectinomycin after overnight incubation at 37°C. Correct integration in the *amyE* gene was confirmed by lack of amylase activity upon growth of the strains on LB plates with 1% starch.

S. pneumoniae strains expressing different *gfp* variants under the zinc-inducible promoter (P_{Zn}) were obtained by transformation of strain R6 (40) with pKB01 derivatives as described previously (28). Correct integration by double crossover was tested by colony PCR using primer pairs integration 1/integration 2 and integration 5/integration 6.

L. lactis strains MG_gfpmut1, MG_gfp+, MG_gfp+htrA, MG_gfp(Sp), MG_sfgfp(Bs), MG_sfgfp(Sp), and MG_sfgfp(iGEM) were obtained by double-crossover integration of plasmids pSEUDO::Pusp45-gfpmut1, pSEUDO::Pusp45-gfp+, pSEUDO::Pusp45-gfp+htrA, pSEUDO::Pusp45-gfp(Sp), pSEUDO::Pusp45-sfgfp(Bs), pSEUDO::Pusp45-GFP_sfgfp(Sp), and pSEUDO::Pusp45-sfgfp(iGEM), respectively, into the pseudo 10 locus on the chromosome of *L. lactis* MG1363. Integration was performed as described by Defoor et al. and Solem et al. (41, 42).

***B. subtilis* growth and GFP expression.** GFP expression in *B. subtilis* was monitored as follows. LB medium with 100 μg ml^{-1} spectinomycin was inoculated with the *B. subtilis amyE*::*gfp* strains directly from the −80°C glycerol stock and grown overnight at 37°C with shaking at 200 rpm. The overnight cultures were diluted 1:50 to an approximate optical density at 600 nm (OD_{600}) of 0.06 in 10 ml fresh Spizizen minimal medium without antibiotics. After growth for 2 h at 37°C, GFP was induced by adding 0.1 mM isopropyl-β-D-1-thiogalactopyranoside (IPTG). After another 2 h of growth, the culture was washed with phosphate-buffered saline (PBS), and fluorescence was measured in a microtiter plate reader and by fluorescence microscopy (see description below). For the latter, cells were concentrated 10 times by centrifugation after which 0.5 μl of cells was spotted onto a microscope slide for the analysis. The slide carried a thin layer of 1% agarose (wt/vol) in PBS covered by a coverslip.

B. subtilis was grown in complex colonies as previously described (27). Briefly, strains were spotted on 2× SG agar plates with 0.1 mM IPTG and incubated at 30°C for 2 days.

***S. pneumoniae* growth and GFP expression.** *S. pneumoniae gfp*-carrying strains and the wild-type R6 strain were grown to an OD_{600} of 0.05 at 37°C in liquid C+Y medium without antibiotics. For induction of expression from P_{Zn}, 0.1 mM $ZnCl_2$ was added to the cells, which were subsequently grown for another 70 min at 37°C. The cells were then harvested and washed with PBS. Fluorescence was determined by using a microtiter plate reader and microscope (see description below). For microscopy, 0.4 μl of the cell suspension was spotted onto a microscope slide carrying a thin layer of 1.2% agarose in PBS covered by a coverslip.

***L. lactis* growth and GFP expression.** GFP-expressing *L. lactis* strains were grown overnight at 30°C in GM17 medium with 1 μg ml^{-1} erythromycin. Overnight cultures were diluted 1:20 in 10 ml of fresh GM17 medium with 1 μg ml^{-1} erythromycin and grown at 30°C until the mid-exponential growth phase. The cells were then harvested and washed with PBS. Fluorescence was determined by using a microtiter plate reader and microscope (see description below). For microscopy, 0.4 μl of the cell suspension was spotted onto a microscope slide carrying a thin layer of 1.2% agarose in PBS covered by a coverslip.

Microtiter plate assays. Cultures of *B. subtilis*, *S. pneumoniae*, and *L. lactis* were grown and prepared as described above. Growth and fluorescence were monitored in microtiter plates at 37°C (*B. subtilis* and *S. pneumoniae*) or 30°C (*L. lactis*) with the following equipment and settings: Infinite 200 plate reader (Tecan Group Ltd.) with I-control 1.7.1.12 software (Tecan Group Ltd.) and GFP filter set (Chroma; excitation at 485 nm [20-nm width] and emission at 535 nm [25-nm width]). GFP signals were collected as top readings with a gain setting of 70. GFP values were corrected for background fluorescence, OD_{600}, and negative controls (values of the wild-type strains). The OD_{600} levels used were corrected for the background value of the corresponding medium used for growth. The calculation used for resolving the relative GFP levels of the cultures is depicted by the following equation:

$$\left(\frac{GFP_{reporter} - GFP_{medium}}{OD_{reporter} - OD_{medium}}\right) - \left(\frac{GFP_{wt} - GFP_{medium}}{OD_{wt} - OD_{medium}}\right)$$

where $GFP_{reporter}$ is the level of GFP of the reporter gene, GFP_{medium} is the level of GFP in the medium, $OD_{reporter}$ is the optical density of the reporter gene, and GFP_{wt} is the level of GFP in the wild type.

Microscopy. Cultures of *B. subtilis*, *S. pneumoniae*, and *L. lactis* were grown and prepared as described above for each organism. Images were taken with an Olympus IX71 microscope (Personal DV, Applied Precision; assembled by Imsol, Preston, United Kingdom) using CoolSNAP HQ2 camera (Princeton Instruments, Trenton, NJ, USA) with a 100× phase-contrast objective. Fluorescence filter sets (excitation, 450 to 490 nm; emission, 500 to 550 nm) used to visualize GFP were from Chroma

Technology Corporation (Bellows Falls, VT, USA). The exposure times were 0.2 s with 32% excitation xenon light (300 W) for *B. subtilis*, 1 s with 100% excitation for *S. pneumoniae*, and 0.8 s with 100% excitation for *L. lactis*. Softworx 3.6.0 (Applied Precision, Issaquah, WA, USA) software was used for image capturing. Phase-contrast images were segmented automatically and analyzed using Microbetracker (43), and cell length distributions and signal intensities were plotted using MATLAB R2011a. Fluorescence levels were corrected for background fluorescence of the medium. Calculation of phenotypic noise strength was done as described in reference 44.

Fluorescence in *B. subtilis* complex colonies was detected using an Olympus MVX10 macro zoom fluorescence microscope equipped with a PreciseExcite light-emitting diode (LED) fluorescence illumination (470 nm), GFP filter set (excitation at 460/480 nm and emission at 495/540 nm), and an Olympus XM10 monochrome camera (Olympus Corporation, Tokyo, Japan).

Nucleotide sequence accession numbers. The DNA sequences of *sfgfp*(Bs) and *sfgfp*(Sp), as well as the other, previously described *gfp* genes, are deposited at NCBI (KF410612 to KF410618).

RESULTS AND DISCUSSION

Selection and design of codon-optimized *gfp* genes. Green fluorescent proteins generally used in molecular biology are mutant variants of the *Aequorea victoria* GFP protein with improved characteristics. Optimizations include codon adaptation of the *gfp* gene to the organism of interest, amino acid modifications or alterations to the folding properties of the protein, or changes to the chromophore (Table 2). For this study, we selected or generated the following GFPs: GFPmut1, GFP+, GFP+(htrA), GFP(Sp), sfGFP(Bs), sfGFP(Sp), and sfGFP(iGEM). A widely used GFP variant for use in bacteria is GFPmut1 (18). Mutations in the chromophore of this protein result in a redshift of the excitation maximum to 488 nm and a 35-fold-higher fluorescence signal compared to the original GFP excited at 488 nm. Folding and maturation of the chromophore are also improved compared to the original GFP, and fluorescence can be detected earlier after induction. The *gfp*+ gene (20) has an *E. coli* codon usage, while the encoded protein carries chromophore and folding mutations, yielding 130-fold-higher fluorescence compared to *A. victoria* GFP. In *gfp*+(htrA), an additional region upstream of *gfp*+ encodes the first three amino acid residues of the *S. pneumoniae* HtrA protein which probably improves ribosome accessibility; GFP+(htrA) was shown to work as a robust reporter for protein fusions and to significantly improve heterologous protein production in *S. pneumoniae* (12, 34). The *S. pneumoniae* codon-optimized *gfp*(Sp) variant specifies a protein with chromophore and folding mutations similar to those in GFPmut2 (36). Dimerization of this GFP at higher concentrations is prevented by the dimer interface-breaking A206K (A at position 206 changed to K) mutation (45), making it very suitable for protein fusions meant to assess intracellular localization. Superfolder GFP (sfGFP) is especially useful for translational fusions, since it rapidly folds and matures even when fused to poorly folding peptides (19, 46). Furthermore, sfGFP might be particularly suitable for gene expression studies, since the emergence of fluorescence closely matches induction of transcription. We employ three sfGFP variants: sfGFP(iGEM), sfGFP(Bs), and sfGFP(Sp), originating from the sfGFP sequences created by Pédelacq et al. (19). sfGFP(iGEM) is a previously characterized variant; the gene was designed for the International Genetically Engineered Machine competition (iGEM) by the University of Cambridge team in 2008, and its codon usage is a compromise for optimum expres-

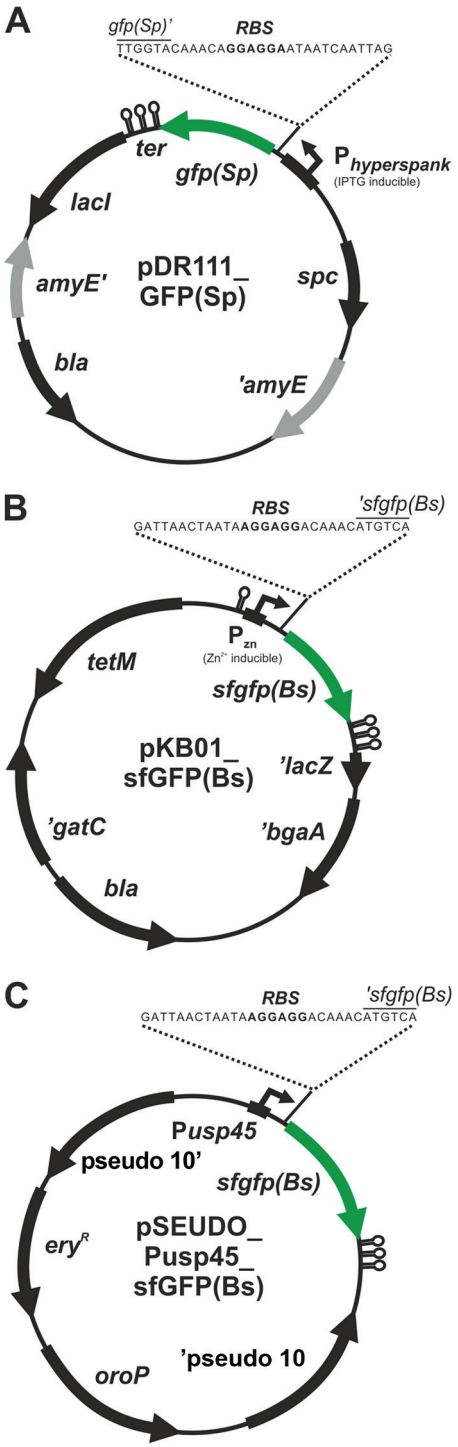

FIG 1 GFP expression vectors for *B. subtilis*, *S. pneumoniae*, and *L. lactis*. (A) Plasmid pDR111_gfp(Sp) integrates in the *B. subtilis* genome at the *amyE* gene locus by double crossover and allows IPTG-inducible expression of *gfp*(*Sp*). (B) Plasmid pKB01_sfgfp(Bs) integrates in the *S. pneumoniae* genome at the *bgaA* gene locus and allows Zn^{2+}-inducible expression of *sfgfp*(*Bs*). (C) Plasmid pSEUDO::Pusp45-sfgfp(Bs) integrates in the *L. lactis* genome at the pseudo 10 gene locus by double crossover, and *sfgfp*(*Bs*) expression is driven by the strong constitutive Pusp45 promoter.

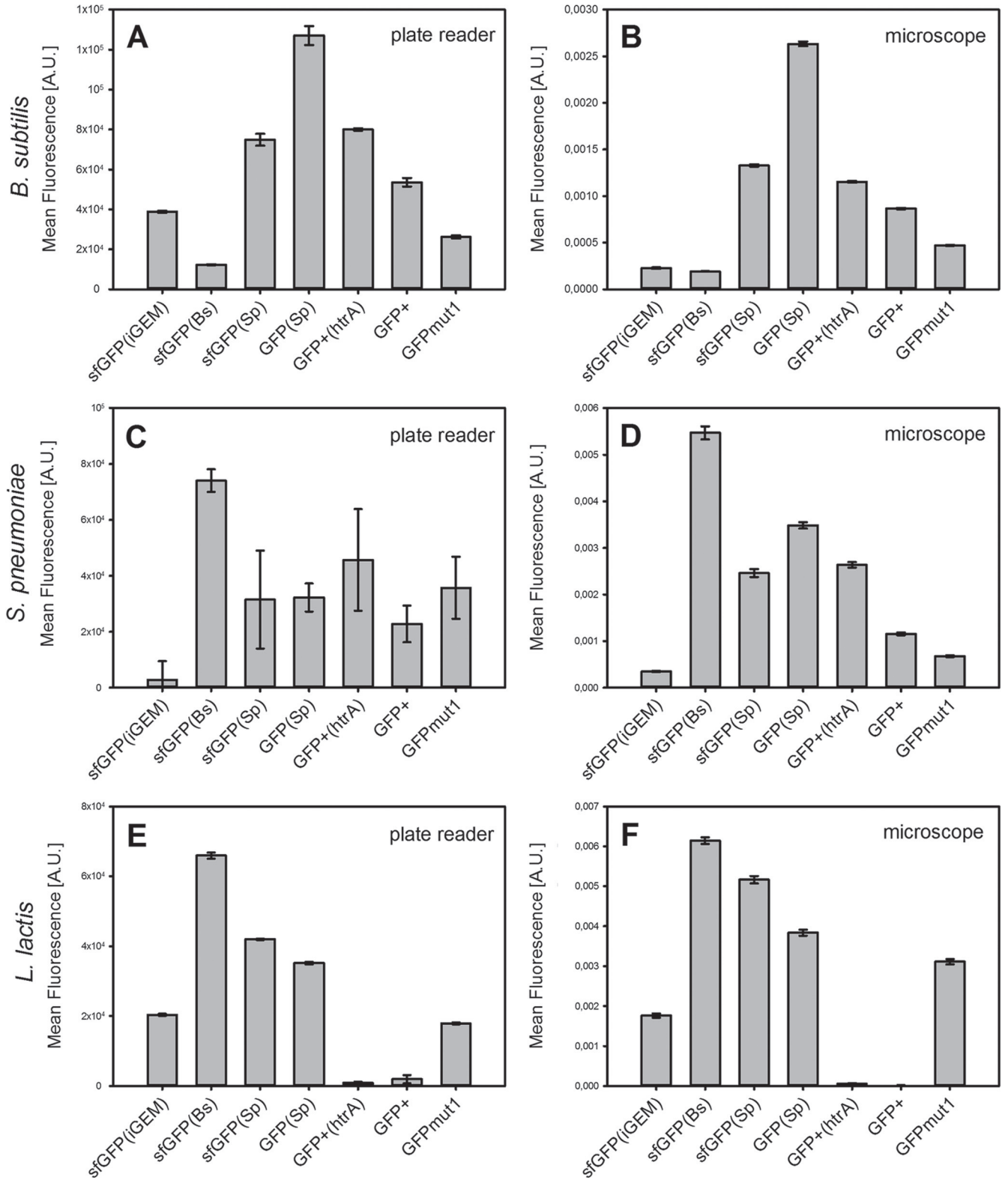

FIG 2 Fluorescence quantification of GFP variants in *B. subtilis* (A and B), *S. pneumoniae* (C and D), and *L. lactis* (E and F). The left panels show population-level GFP signals recorded using microtiter plate readings. Fluorescence intensities are corrected for background fluorescence, OD_{600}, and wild-type strain (no GFP) values. Error bars indicate the standard errors of the means ($n \geq 3$). Simultaneously, single-cell fluorescence was measured in the same cultures with fluorescence microscopy (right panels). Fluorescence intensities are normalized for background fluorescence, cell area, and wild-type strain values. Error bars indicate the standard errors of the means ($n \geq 200$). Note that fluorescence values from both methods are in arbitrary units (A.U.) and are not directly comparable.

sion in *E. coli* and *B. subtilis* (46). In addition, sfGFP(iGEM) carries the mutations S2R and S72A from GFPmut3* (47). No phenotypic effects have been reported for S2R, while the S72A folding mutation close to the chromophore enhances fluorescence (47). To be able to optimally use sfGFP in *B. subtilis* and *S. pneumoniae*, we designed and synthesized codon-optimized genes for sfGFP variants, *sfgfp*(*Bs*) and *sfgfp*(*Sp*), respectively (see Materials and Methods). With the design of two new *sfgfp* genes, the total number of GFP variants benchmarked in this study is seven.

Construction of new GFP vectors for *B. subtilis*, *S. pneumoniae*, and *L. lactis*. To evaluate the seven GFPs for their production and fluorescence properties, we constructed new GFP vectors for integration into the chromosome of each of the three model organisms. It is important to note that for each organism the GFP variants are expressed using the same promoter and ribosome binding site (RBS), allowing direct comparisons. For *B. subtilis*, plasmid pDR111 (a kind gift from David Rudner) was used as the replicon. This vector is a derivative of the Pspac-hy plasmid pJQ43 (48), which achieves better repression in the absence of the IPTG inducer due to an extra *lacO* operator site (33). PCR fragments carrying *gfp* constructs were cloned downstream of the $P_{hyperspank}$ promoter region. The PCR fragments included three stop codons in the 3 different reading frames and a RBS upstream of the *gfp* gene and three terminators downstream of the *gfp* gene to terminate transcription and prevent read-through transcription from downstream genes (Fig. 1A). The regions of the *amyE* gene flanking the *gfp* genes facilitate integration at the *amyE* locus in the *B. subtilis* chromosome. Ampicillin and spectinomycin resistance cassettes are present to allow selection in *E. coli* and *B. subtilis*, respectively. The setup chosen guarantees that each of the seven *gfp* genes is located in exactly the same genetic surrounding.

S. pneumoniae plasmid pKB01_*sfgfp*(*Bs*) (Fig. 1B) was constructed by introducing the Zn^{2+}-inducible promoter P_{Zn} and *sfgfp*(*Bs*) into plasmid pJWV100 which is flanked by transcriptional terminators as described in Materials and Methods. The Zn^{2+}-inducible promoter P_{Zn} allows tight regulation of *gfp* expression (12). The flanking regions of the nonessential *bgaA* gene facilitate integration at this locus in the *S. pneumoniae* chromosome. A tetracycline resistance cassette allows for selection in *S. pneumoniae*. All other *gfp*-carrying pKB01 vectors were constructed in the same way.

L. lactis plasmid pSEUDO::Pusp45-*sfgfp*(*Bs*) (Fig. 1C) was constructed by introducing Pusp45 and *sfgfp*(*Bs*) into pSEUDO-GFP. The strong constitutive *usp45* promoter of *L. lactis* MG1363 (49) drives expression of *gfp*. Three terminators downstream of the *gfp* gene terminate transcription and prevent read-through transcription from downstream genes. The regions of the pseudo 10 gene flanking the *gfp* gene facilitate integration at the pseudo 10 locus in the *L. lactis* chromosome (38). An erythromycin resistance cassette allows for selection in *L. lactis*. All other *gfp*-carrying pSEUDO::Pusp45 derivatives were constructed in the same way.

Characterization of GFP expression at the population level. Strains of *B. subtilis*, *S. pneumoniae*, and *L. lactis* were cultured in 96-well microtiter plates and examined for GFP fluorescence. Additionally, fluorescence was determined in *B. subtilis* complex colonies. Results are shown in Fig. 2 and 3.

(i) *Bacillus subtilis*. Strikingly, in *B. subtilis*, *gfp*(Sp) carrying codon optimizations for *S. pneumoniae* exhibited the strongest fluorescence signal; the average signals were approximately 5-fold higher than when the widely used GFPmut1 was expressed (18, 35) (Fig. 2A). The fluorescent proteins sfGFP(Sp), GFP+(htrA), and GFP+ also exhibited a signal stronger than that of GFPmut1. Unlike what was expected, sfGFP(Bs) performed worst in the host for which the gene was codon optimized, *B. subtilis*. While the protein sequences of sfGFP(Bs) and sfGFP(Sp) are identical, the fluorescence level of the latter in *B. subtilis* is 6- to 7-fold higher. At the DNA level, sfGFP(Bs) and sfGFP(Sp) show 20% dissimilarity, illustrating the impact of codon usage on heterologous protein production. Fluorescence data of complex *B. subtilis* colonies show that the relative GFP signals under these circumstances are comparable to those of planktonic conditions (Fig. 3). GFP(Sp) gave the highest signals, followed by sfGFP(Sp) and GFP+(htrA). Thus, even in biofilms, in which cells are less well aerated than in shaken planktonic cultures, the nonsuperfolder GFP(Sp) outperforms the other variants.

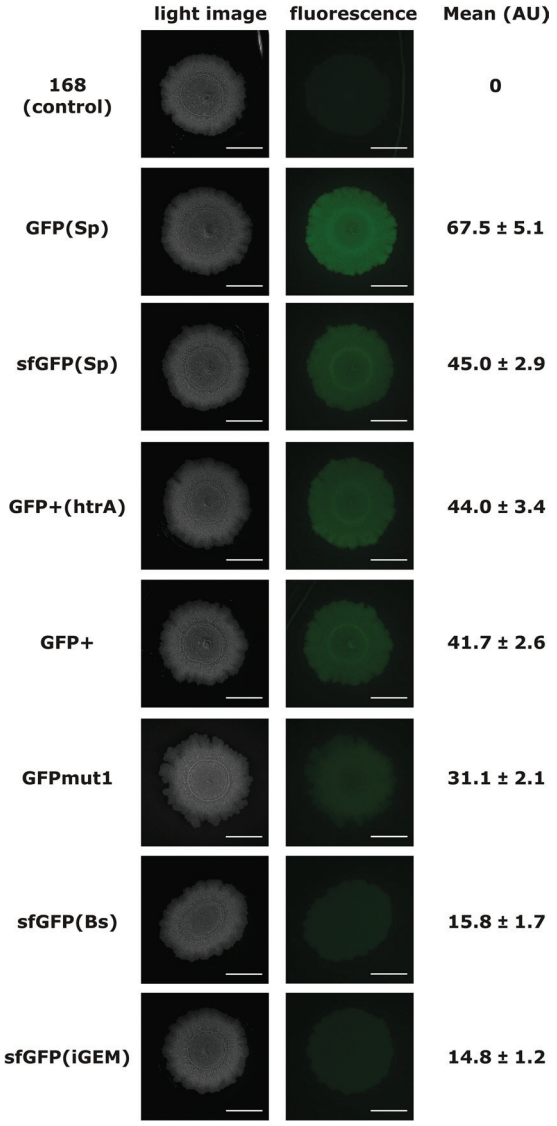

FIG 3 Detection of architecturally complex colony development (left) and GFP levels (right) in various *B. subtilis* strains grown on 2× SG medium. The strain name or GFP variant is indicated to the left of the images, while the mean fluorescence (in arbitrary units [AU]) of various strains detected with CellP software (Olympus) is indicated to the right of the images. Bars, 10 mm.

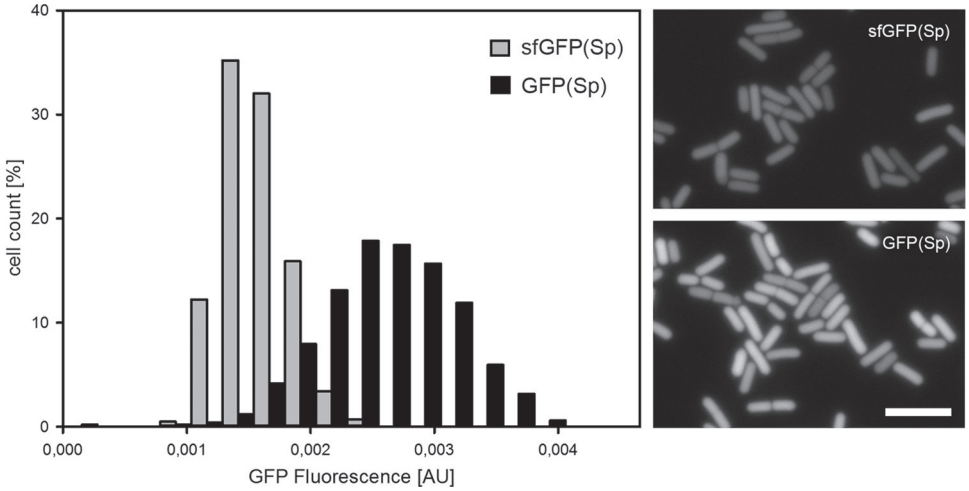

FIG 4 GFP fluorescence signal distribution. The fluorescence intensity frequencies of GFP(Sp) and sfGFP(Sp) in *B. subtilis* are plotted. While the mean signal of sfGFP(Sp) is higher, it is distributed over a wider range of intensities than sfGFP(Sp). Micrograph examples of the two strains are shown on the right. Bar, 5 μm.

(ii) *Streptococcus pneumoniae.* In *S. pneumoniae*, sfGFP(Bs) exhibited the highest fluorescence signal of all GFPs tested (Fig. 2C). The gene of this superfolder GFP variant is codon optimized for *B. subtilis*. It performed remarkably better than the same gene codon optimized for *S. pneumoniae*. Note that different codon optimization strategies were used for sfGFP(Bs) and sfGFP(Sp) (see Materials and Methods), so we cannot formally conclude which codon optimization strategy is superior for which organism. Nevertheless, the signal of sfGFP(Bs) was roughly two times stronger than that of sfGFP(Sp), GFP(Sp), and GFPmut1 when expressed in *S. pneumoniae*. GFP+(htrA) exhibited a stronger fluorescence signal than GFP+. The GFP signal increased by a factor of two by the sole introduction of the 3 *htrA* codons to the 5′ end of *gfp*+, as has been described previously in the case of expression of LacZ (34). The weakest fluorescence was exhibited by sfGFP(iGEM) with a signal that was barely detectable above autofluorescence.

(iii) *Lactococcus lactis.* The relative fluorescence levels of the seven GFPs in *L. lactis* (Fig. 2E) are comparable to those in *S. pneumoniae*. With GFP+ and GFP+(htrA) as the exceptions, a similar ranking based on fluorescence intensities can be made. The fluorescence signals of both GFP+ and GFP+(htrA) are hardly above autofluorescence, which makes them unsuitable for use in *L. lactis*. The best-performing GFP in this organism is sfGFP(Bs), with a signal approximately 3.5-fold higher than those of GFPmut1 and sfGFP(iGEM). Runners-up are the two GFPs for which the genes were codon optimized for *S. pneumoniae*, with the superfolder variant producing slightly more fluorescence signal.

Altogether these results demonstrate that for the conditions tested, a GFP with a strong fluorescence at the population level can be selected for each organism: GFP(Sp) for planktonic and biofilm cells of *B. subtilis* and sfGFP(Bs) for both *S. pneumoniae* and *L. lactis*.

Characterization of GFP expression at the single-cell level. Fluorescence microscopy was performed to examine the signal of each GFP reporter at the single-cell level. Single-cell GFP signals were quantified using Microbetracker (43). Simultaneously, population-level GFP signals were recorded on the same cultures using microtiter plate readings. Results are shown in Fig. 2. In general, the average fluorescence observed in the single-cell assays correlated well with the data of the population-wide microtiter plate assays. In *B. subtilis*, the only GFP that deviates from the trend found in the microtiter plate assays is sfGFP(iGEM) (Fig. 2B). Its fluorescence signal is twofold lower than that of GFPmut1, making it, together with sfGFP(Bs), the GFP with the least fluorescence. The GFP variant generating the highest fluorescence signals is, again, GFP(Sp) with an average fluorescence almost 2-fold higher than that of sfGFP(Sp), the second best GFP.

As with the microtiter plate assay, sfGFP(Bs) gives the highest fluorescence signal in single cells from *S. pneumoniae* (Fig. 2D), namely, approximately two times higher than that of sfGFP(Sp) and six times higher than that of GFPmut1.

The single-cell results obtained with *L. lactis* are nearly identical to those on the population level: in both cases, sfGFP(Bs) is the best GFP under the experimental conditions employed here (Fig. 2F). Its signal is roughly twice higher than that of GFPmut1. GFP+ and GFP+(htrA) are barely detectable, even with the sensitive method of fluorescence microscopy.

The data obtained from bulk cultures do not reflect the situation at the single-cell level in every case. When the data are plotted as a histogram, it becomes evident that the fluorescence signal is not equal in all cells and that the amount of signal variation among cells differs per GFP variant. From the histograms of *B. subtilis* GFP(Sp) and sfGFP(Sp) for example, it is clear that the GFP(Sp) signal is much broader than that of sfGFP(Sp) (Fig. 4). See Fig. S1 for all GFP signal distributions.

Phenotypic noise. As observed above in the single-cell analyses, GFP signals may vary among individual cells. In some experimental setups, it is crucial that the GFP fluorescence signal is homogeneous, for example when studying phenotypic heterogeneity using promoter-GFP fusions as reporters for gene expression. In those cases, one needs to be confident that variation in fluorescence signal originates from promoter activity, not from an intrinsic property of the GFP employed.

Thus, we quantified the spread in a population of expression levels of the various GFPs studied here. The distribution of gene

TABLE 3 Phenotypic noise strength

GFP	Phenotypic noise strength[a]		
	B. subtilis	*S. pneumoniae*	*L. lactis*
GFPmut1	0.33	3.66	37.66
GFP+	0.87	8.11	12.28
GFP+(*htrA*)	1.26	24.70	10.68
GFP(*Sp*)	7.24	27.77	46.06
sfGFP(*Bs*)	0.16	75.90	59.83
sfGFP(*Sp*)	2.24	51.90	86.50
sfGFP(iGEM)	0.38	1.25	35.27

[a] Calculations of phenotypic noise strength were done by the method of Ozbudak et al. (44). All values are multiplied by 10^5.

expression of a single gene can be described by a mean value of expression (as measured by GFP signal) indicated by $<p>$ with a standard deviation, σ_p. The Fano factor ($\sigma_p^2/<p>$), or phenotypic noise strength, is a commonly used measure of noise (44, 50, 51). This measure is used because the relative standard deviation changes as the mean value changes, whereas the phenotypic noise strength is less sensitive to changes in the mean value. The Fano factor is thus a measure of noise that allows relative comparison of gene expression distributions among populations (44, 50, 51).

The general trend for the GFPs benchmarked in this study is that phenotypic noise strength is proportional to fluorescence signal (Table 3). The GFP generating the highest fluorescence signals in *B. subtilis*, GFP(Sp), shows the most heterogeneous fluorescence at the single-cell level. Also in *S. pneumoniae*, the GFP with the highest fluorescence signal, sfGFP(Bs), exhibits the highest phenotypic noise. In *L. lactis*, however, the GFP with the highest fluorescence signal, sfGFP(Bs), does not have the strongest phenotypic noise: sfGFP(Bs) exhibits the strongest fluorescence signal, but its phenotypic noise levels are below that of the weaker fluorescing sfGFP(Sp). This makes sfGFP(Bs) a very suitable marker to study gene expression at the single-cell level in *L. lactis*.

The sources for the observed differences in phenotypic noise are unclear but might involve cell-to-cell variability in protein synthesis (transcription and translation), mRNA stability, GFP maturation and/or folding and are thus of crucial importance to take into account when examining single-cell gene expression patterns.

Concluding remarks. Seven GFP variants have been benchmarked with respect to fluorescence signal strength in *B. subtilis*, *S. pneumoniae*, and *L. lactis* on both the level of the population and the single cell. To this end, new *gfp* vectors for genomic integration were constructed. Our results allow a clear ranking of the GFPs based on their fluorescence signals. The GFPs generating the highest fluorescence signals for *B. subtilis*, *S. pneumoniae*, and *L. lactis* are GFP(Sp), sfGFP(Bs), and sfGFP(Bs), respectively. It is important to note that this ranking is likely influenced by the choice of the RBS and that each gene might be expressed differently with a different RBS (32, 52). The importance of the 5′ end of the transcript for total protein production is well-known. For instance, without the need to completely codon optimize the entire gene, expression of fluorescent protein production could be tremendously improved by adding a few codons of a gene of a well-expressed protein to the 5′ end of the gene encoding the fluorescent protein in both *B. subtilis* and *S. pneumoniae*, which likely improves ribosome accessibility to the RBS, thus improving translation (53, 54).

In general, the underlying molecular mechanisms for the large differences in GFP signals between the seven GFP variants in the different organisms are unclear at this moment and lie outside the scope of this work. Besides the specific mutations in the various GFPs, the large differences might be related to mRNA stability, translation efficiency, GFP-folding efficiency, chromophore maturation, and protein stability. Nevertheless, this work provides a good basis for selecting a proper GFP variant for each of these widely used low-GC Gram-positive model species.

ACKNOWLEDGMENTS

We thank David Rudner for the kind gift of plasmid pDR111 and Nathalie Campo for kindly providing plasmid pUC57-gfp(opt). We thank Hans Roubos (DSM) for kindly providing the *sfgfp*(Bs) sequence.

Work in Oscar P. Kuipers' lab was supported by an STW grant (107504) to support Ana Solopova and an ALW grant (81807004) to support Ákos T. Kovács. Wout Overkamp is supported by a grant from the Kluyver Centre for Genomics of Industrial Fermentation, which is part of the Netherlands Genomics Initiative/Netherlands Organization for Scientific Research (NWO). Ruud Detert Oude Weme is supported by a Sysmo2 grant to Oscar P. Kuipers. Work in Jan-Willem Veening's lab is funded by a Veni fellowship and by a Sysmo2 grant ("NoisyStrep") both from NWO-ALW (Earth and Life Sciences).

REFERENCES

1. **Southward CM, Surette MG.** 2002. The dynamic microbe: green fluorescent protein brings bacteria to light. Mol. Microbiol. **45:**1191–1196.
2. **Valdivia RH, Cormack BP.** 2005. The uses of green fluorescent protein in prokaryotes. Methods Biochem. Anal. **47:**163–178.
3. **Dubnau D.** 1991. Genetic competence in *Bacillus subtilis*. Microbiol. Rev. **55:**395–424.
4. **Errington J.** 2003. Regulation of endospore formation in *Bacillus subtilis*. Nat. Rev. Microbiol. **1:**117–126.
5. **Kearns DB, Losick R.** 2005. Cell population heterogeneity during growth of *Bacillus subtilis*. Genes Dev. **19:**3083–3094.
6. **Msadek T.** 1999. When the going gets tough: survival strategies and environmental signaling networks in *Bacillus subtilis*. Trends Microbiol. **7:**201–207.
7. **Veening J-W, Smits WK, Kuipers OP.** 2008. Bistability, epigenetics, and bet-hedging in bacteria. Annu. Rev. Microbiol. **62:**193–210.
8. **Branda SS, González-Pastor JE, Ben-Yehuda S, Losick R, Kolter R.** 2001. Fruiting body formation by *Bacillus subtilis*. Proc. Natl. Acad. Sci. U. S. A. **98:**11621–11626.
9. **Kadioglu A, Weiser JN, Paton JC, Andrew PW.** 2008. The role of *Streptococcus pneumoniae* virulence factors in host respiratory colonization and disease. Nat. Rev. Microbiol. **6:**288–301.
10. **Scott JAG, Brooks WA, Peiris JSM, Holtzman D, Mulhollan EK.** 2008. Pneumonia research to reduce childhood mortality in the developing world. J. Clin. Invest. **118:**1291–1300.
11. **Beilharz K, Nováková L, Fadda D, Branny P, Massidda O, Veening J-W.** 2012. Control of cell division in *Streptococcus pneumoniae* by the conserved Ser/Thr protein kinase StkP. Proc. Natl. Acad. Sci. U. S. A. **109:**E905–E913.
12. **Eberhardt A, Wu LJ, Errington J, Vollmer W, Veening J-W.** 2009. Cellular localization of choline-utilization proteins in *Streptococcus pneumoniae* using novel fluorescent reporter systems. Mol. Microbiol. **74:**395–408.
13. **de Jong IG, Beilharz K, Kuipers OP, Veening J-W.** 2011. Live cell imaging of *Bacillus subtilis* and *Streptococcus pneumoniae* using automated time-lapse microscopy. J. Vis. Exp. **2011:**e3145. doi:10.3791/3145.
14. **Sham L-T, Barendt SM, Kopecky KE, Winkler ME.** 2011. Essential PcsB putative peptidoglycan hydrolase interacts with the essential FtsXSpn cell division protein in *Streptococcus pneumoniae* D39. Proc. Natl. Acad. Sci. U. S. A. **108:**E1061–E1069.
15. **Campelo AB, Rodriguez A, Martinez B.** 2010. Use of green fluorescent protein to monitor cell envelope stress in *Lactococcus lactis*. Appl. Environ. Microbiol. **76:**978–981.
16. **Chalfie M, Tu Y, Euskirchen G, Ward WW, Prasher DC.** 1994. Green fluorescent protein as a marker for gene expression. Science **263:**802–805.

17. **Geoffroy M-C, Guyard C, Quatannens B, Pavan S, Lange M, Mercenier A.** 2000. Use of green fluorescent protein to tag lactic acid bacterium strains under development as live vaccine vectors. Appl. Environ. Microbiol. **66:**383–391.
18. **Cormack BP, Valdivia RH, Falkow S.** 1996. FACS-optimized mutants of the green fluorescent protein (GFP). Gene **173:**33–38.
19. **Pédelacq J-D, Cabantous S, Tran T, Terwilliger TC, Waldo GS.** 2006. Engineering and characterization of a superfolder green fluorescent protein. Nat. Biotechnol. **24:**79–88.
20. **Scholz O, Thiel A, Hillen W, Niederweis M.** 2000. Quantitative analysis of gene expression with an improved green fluorescent protein. Eur. J. Biochem. **267:**1565–1570.
21. **Shaner NC, Steinbach PA, Tsien RY.** 2005. A guide to choosing fluorescent proteins. Nat. Methods **2:**905–909.
22. **Lithwick G, Margalit H.** 2003. Hierarchy of sequence-dependent features associated with prokaryotic translation. Genome Res. **13:**2665–2673.
23. **Moszer I, Rocha EP, Danchin A.** 1999. Codon usage and lateral gene transfer in *Bacillus subtilis*. Curr. Opin. Microbiol. **2:**524–528.
24. **Gustafsson C, Govindarajan S, Minshull J.** 2004. Codon bias and heterologous protein expression. Trends Biotechnol. **22:**346–353.
25. **Sambrook J, Fritsch EF, Maniatis T.** 1989. Molecular cloning: a laboratory manual. Cold Spring Harbor Laboratory, Cold Spring Harbor, NY.
26. **Anagnostopoulos C, Spizizen J.** 1961. Requirements for transformation in *Bacillus subtilis*. J. Bacteriol. **81:**741–746.
27. **Kovács AT, Kuipers OP.** 2011. Rok regulates *yuaB* expression during architecturally complex colony development of *Bacillus subtilis* 168. J. Bacteriol. **193:**998–1002.
28. **Martin B, García P, Castanié MP, Claverys JP.** 1995. The *recA* gene of *Streptococcus pneumoniae* is part of a competence-induced operon and controls lysogenic induction. Mol. Microbiol. **15:**367–379.
29. **Harwood CR, Cutting SM.** 1990. Molecular biological methods for *Bacillus*. John Wiley & Sons, Hoboken, NJ.
30. **Holo H, Nes IF.** 1995. Transformation of *Lactococcus* by electroporation. Methods Mol. Biol. **47:**195–199.
31. **Puigbò P, Guzmán E, Romeu A, Garcia-Vallvé S.** 2007. OPTIMIZER: a web server for optimizing the codon usage of DNA sequences. Nucleic Acids Res. **35:**W126–W131.
32. **de Smit MH, van Duin J.** 1990. Secondary structure of the ribosome binding site determines translational efficiency: a quantitative analysis. Proc. Natl. Acad. Sci. U. S. A. **87:**7668–7672.
33. **Britton RA, Eichenberger P, Gonzalez-Pastor JE, Fawcett P, Monson R, Losick R, Grossman AD.** 2002. Genome-wide analysis of the stationary-phase sigma factor (sigma-H) regulon of *Bacillus subtilis*. J. Bacteriol. **184:**4881–4890.
34. **Halfmann A, Hakenbeck R, Brückner R.** 2007. A new integrative reporter plasmid for *Streptococcus pneumoniae*. FEMS Microbiol. Lett. **268:**217–224.
35. **Lewis PJ, Marston AL.** 1999. GFP vectors for controlled expression and dual labelling of protein fusions in *Bacillus subtilis*. Gene **227:**101–109.
36. **Martin B, Granadel C, Campo N, Hénard V, Prudhomme M, Claverys J-P.** 2010. Expression and maintenance of ComD–ComE, the two-component signal-transduction system that controls competence of *Streptococcus pneumoniae*. Mol. Microbiol. **75:**1513–1528.
37. **Milde S.** 2008. Superfold GFP driven by T7 promoter. Part:BBa_I746909. iGEM Registry of Standard Biological Parts. The International Genetically Engineered Machine (iGEM) Foundation, Cambridge, MA, USA.
38. **Pinto JPC, Zeyniyev A, Karsens H, Trip H, Lolkema JS, Kuipers OP, Kok J.** 2011. pSEUDO, a genetic integration standard for *Lactococcus lactis*. Appl. Environ. Microbiol. **77:**6687–6690.
39. **Kunst F, Ogasawara N, Moszer I, Albertini AM, Alloni G, Azevedo V, Bertero MG, Bessières P, Bolotin A, Borchert S, Borriss R, Boursier L, Brans A, Braun M, Brignell SC, Bron S, Brouillet S, Bruschi CV, Caldwell B, Capuano V, Carter NM, Choi SK, Codani JJ, Connerton IF, Cummings NJ, Daniel RA, Denizot F, Devine KM, Düsterhöft A, Ehrlich SD, Emmerson PT, Entian KD, Errington J, Fabret C, Ferrari E, Foulger D, Fritz C, Fujita M, Fujita Y, Fuma S, Galizzi A, Galleron N, Ghim S-Y, Glaser P, Goffeau A, Golightly EF, Grandi G, Guiseppi G, Guy BJ, Haga K, et al.** 1997. The complete genome sequence of the gram-positive bacterium *Bacillus subtilis*. Nature **390:**249–256.
40. **Hoskins J, Alborn WE, Jr, Arnold J, Blaszczak LC, Burgett S, DeHoff BS, Estrem ST, Fritz L, Fu DJ, Fuller W, Geringer C, Gilmour R, Glass JS, Khoja H, Kraft AR, Lagace RE, LeBlanc DJ, Lee LN, Lefkowitz EJ, Lu J, Matsushima P, McAhren SM, McHenney M, McLeaster K, Mundy CW, Nicas TI, Norris FH, O'Gara M, Peery RB, Robertson GT, Rockey P, Sun PM, Winkler ME, Yang Y, Young-Bellido M, Zhao G, Zook CA, Baltz RH, Jaskunas SR, Rosteck PR, Jr, Skatrud PL, Glass JI.** 2001. Genome of the bacterium *Streptococcus pneumoniae* strain R6. J. Bacteriol. **183:**5709–5717.
41. **Defoor E, Kryger M-B, Martinussen J.** 2007. The orotate transporter encoded by *oroP* from *Lactococcus lactis* is required for orotate utilization and has utility as a food-grade selectable marker. Microbiology (Reading, Engl.) **153:**3645–3659.
42. **Solem C, Defoor E, Jensen PR, Martinussen J.** 2008. Plasmid pCS1966, a new selection/counterselection tool for lactic acid bacterium strain construction based on the *oroP* gene, encoding an orotate transporter from *Lactococcus lactis*. Appl. Environ. Microbiol. **74:**4772–4775.
43. **Sliusarenko O, Heinritz J, Emonet T, Jacobs-Wagner C.** 2011. High-throughput, subpixel precision analysis of bacterial morphogenesis and intracellular spatio-temporal dynamics. Mol. Microbiol. **80:**612–627.
44. **Ozbudak EM, Thattai M, Kurtser I, Grossman AD, van Oudenaarden A.** 2002. Regulation of noise in the expression of a single gene. Nat. Genet. **31:**69–73.
45. **Zacharias DA, Violin JD, Newton AC, Tsien RY.** 2002. Partitioning of lipid-modified monomeric GFPs into membrane microdomains of live cells. Science **296:**913–916.
46. **Milde S, Brown J, Schmidt H, Boettger L, Chapart M, Cheng K, Chung K, Goodman D, Hill C, Koeningsberg-Miles R, Mehta A, Myelnikov D, O'Neill E, Tang I, Wu J, Yan X-H.** 2008. Improved GFP. iGEM Registry of Standard Biological Parts. The International Genetically Engineered Machine (iGEM) Foundation, Cambridge, MA, USA. http://2008.igem.org/Team:Cambridge/Improved_GFP.
47. **Andersen JB, Sternberg C, Poulsen LK, Bjorn SP, Givskov M, Molin S.** 1998. New unstable variants of green fluorescent protein for studies of transient gene expression in bacteria. Appl. Environ. Microbiol. **64:**2240–2246.
48. **Quisel JD, Burkholder WF, Grossman AD.** 2001. In vivo effects of sporulation kinases on mutant Spo0A proteins in *Bacillus subtilis*. J. Bacteriol. **183:**6573–6578.
49. **van Asseldonk M, Rutten G, Oteman M, Siezen RJ, de Vos WM, Simons G.** 1990. Cloning of *usp45*, a gene encoding a secreted protein from *Lactococcus lactis* subsp. *lactis* MG1363. Gene **95:**155–160.
50. **Kaern M, Blake WJ, Collins JJ.** 2003. The engineering of gene regulatory networks. Annu. Rev. Biomed. Eng. **5:**179–206.
51. **Thattai M, van Oudenaarden A.** 2001. Intrinsic noise in gene regulatory networks. Proc. Natl. Acad. Sci. U. S. A. **98:**8614–8619.
52. **Salis HM, Mirsky EA, Voigt CA.** 2009. Automated design of synthetic ribosome binding sites to control protein expression. Nat. Biotechnol. **27:**946–950.
53. **Henriques MX, Catalão MJ, Figueiredo J, Gomes JP, Filipe SR.** 2013. Construction of improved tools for protein localization studies in *Streptococcus pneumoniae*. PLoS One **8:**e55049. doi:10.1371/journal.pone.0055049.
54. **Veening J-W, Smits WK, Hamoen LW, Jongbloed JDH, Kuipers OP.** 2004. Visualization of differential gene expression by improved cyan fluorescent protein and yellow fluorescent protein production in *Bacillus subtilis*. Appl. Environ. Microbiol. **70:**6809–6815.
55. **Puigbo P, Guzman E, Romeu A, Garcia-Vallve S.** 2007. OPTIMIZER: a web server for optimizing the codon usage of DNA sequences. Nucleic Acids Res. **35:**W126–W131.
56. **Gasson MJ.** 1983. Plasmid complements of *Streptococcus lactis* NCDO 712 and other lactic streptococci after protoplast-induced curing. J. Bacteriol. **154:**1–9.